

ber of levels is an unknown amount greater than N .

The present confidence-interval approach to the analysis is the one which we finally considered to be most appropriate for this problem. We initially explored various Bayes theorem approaches where one has the problem of choosing the appropriate *a priori* distribution form and where the expressions are plagued with infinities for small N . We also explored the maximum-likelihood approach and finally rejected it for reasons discussed in the text. As a final comment, it should be noted that our experimental studies^{4,2} strongly support the O.E. theory only for level spacings for favorable cases in the $150 \leq A \leq 190$ mass region. It is not assured that the theory should apply to lighter nuclei or nuclei near closed

shells where $\langle D \rangle$ is very large and where conditions may not yet be appropriate for such an extreme statistical treatment.

ACKNOWLEDGMENTS

The authors wish to thank Dr. H. S. Camarda for his earlier work on generating the correlated level spacings in accord with O.E. which are indispensable to obtaining the Monte Carlo results of this paper. We also thank Dr. G. Hacken, Dr. F. Rahn, and Dr. M. Slagowitz for useful discussion. The contributions of Dr. Freeman Dyson to our earlier treatments of O.E. theory were essential in making this work possible, although we have not discussed the material of this paper with him before publication.

*Research supported in part by the U. S. Atomic Energy Commission.

¹H. I. Liou, H. S. Camarda, S. Wynchank, M. Slagowitz, G. Hacken, F. Rahn, and J. Rainwater, *Phys. Rev. C* **5**, 974 (1972).

²H. S. Camarda, H. I. Liou, F. Rahn, G. Hacken, M. Slagowitz, W. W. Havens, Jr., J. Rainwater, and S. Wynchank, in *Statistical Properties of Nuclei*, edited

by J. B. Garg (Plenum, New York, 1972), pp. 205–213.

³F. J. Dyson and M. L. Mehta, *J. Math. Phys.* **4**, 701 (1963).

⁴H. V. Muradyan and Y. V. Adamchuk, *Nucl. Phys.* **68**, 549 (1965).

⁵D. D. Slavinskas and T. J. Kennett, *Nucl. Phys.* **85**, 641 (1966).

Isospin-Forbidden and Allowed $^{12}\text{C}(d, \alpha)^{10}\text{B}$ Cross Sections*

H. Vernon Smith, Jr.

The University of Wisconsin, Madison, Wisconsin 53706

(Received 10 January 1972)

We report extensive new data on the isospin-forbidden reaction $^{12}\text{C}(d, \alpha_2)^{10}\text{B}(1.74)$ for $7.19 \text{ MeV} \leq E_d \leq 13.99 \text{ MeV}$. We also report extensive data for the isospin-allowed reactions $^{12}\text{C}(d, \alpha_{0,1,3})^{10}\text{B}$. All channels exhibit resonant behavior indicative of compound-nucleus formation. We find no evidence for appreciable direct or semidirect contribution to the α_2 cross sections. A partial-wave expansion of the α_2 data fixes J^π for a number of (isospin-mixed) ^{14}N compound-nuclear levels. Our data do not support either Noble's proposed ^6Li mechanism or Weller's modification to Noble's proposal.

I. INTRODUCTION

Since the deuteron, the α particle, and the ground state of ^{12}C all have zero isospin ($T=0$), and the second excited state of $^{10}\text{B}(1.74 \text{ MeV}, J^\pi = 0^+)$ has $T=1$, the reaction $^{12}\text{C}(d, \alpha_2)^{10}\text{B}(1.74)$ is isospin-forbidden. Thus, if the isospin quantum number is strictly conserved in nuclear reactions, the yield for this reaction is zero. Substantial

cross sections for this and other isospin-forbidden reactions occur,¹⁻¹² and are generally attributed to isospin mixing by Coulomb forces in the compound-nuclear states. However, Meyer-Schützmeister, von Ehrenstein, and Allas² and Jänecke *et al.*^{3,12} suggest that their $^{12}\text{C}(d, \alpha_2)^{10}\text{B}$ data require a direct mechanism. Also Jänecke *et al.*^{5,12} believe their $^{16}\text{O}(d, \alpha_1)^{14}\text{N}(2.31)$ data imply a direct or semidirect mechanism. Since direct

nuclear reactions should conserve isospin (the collision times are so short that the Coulomb forces will not appreciably mix states of different isospin¹³⁻¹⁵), the proposal that isospin nonconservation occurs via a direct mechanism requires careful examination. We therefore investigate the reported direct behavior of the reaction $^{12}\text{C}(d, \alpha_2)^{10}\text{B}$ for $11.3 \text{ MeV} \leq E_d \leq 14.0 \text{ MeV}$.^{2,3} In addition, we repeat and extend the previous measurements for $7.2 \text{ MeV} \leq E_d \leq 11.3 \text{ MeV}$ to study in greater detail the compound mechanism reported for this region² and to search for mirror cluster states in ^{14}N similar to those found in ^8Be .¹⁶ (Such mirror cluster states can explain relatively large isospin mixing observed in a reaction of this type.)

The direct mechanisms proposed^{2,3,17-20} to explain the previous $^{12}\text{C}(d, \alpha_2)^{10}\text{B}$ results generally do not permit cross sections of the magnitude which the data require and, in particular, do not account for the two resonant-like maxima which Ref. 3 reports in a forward-angle excitation function (Fig. 4 of Ref. 3). Noble proposes²¹ a second-order direct process to explain the two resonant maxima. He suggests that the incoming deuteron picks up an α particle from the ^{12}C target, forming ^6Li in one of its two (supposedly isospin-mixed) $J^\pi = 2^+$ states ($E_x = 4.57 \text{ MeV}$, $T=0$ and $E_x = 5.36 \text{ MeV}$, $T=1$), leaving a residual nucleus, ^8Be . The $^6\text{Li}^*(2^+)$ then decays into a singlet deuteron, d , and an α parti-

cle. The ^8Be nucleus absorbs the d , forming $^{10}\text{B}(1.74, J^\pi = 0^+, T=1)$ and leaving the detected α particle. The two resonant-like peaks result from E_d assuming values suitable for forming the 2^+ states in ^6Li , which constitute a $T=0, T=1$ doublet. The existence of bands of cluster states near two-particle breakup thresholds²² plus the possibility of appreciable isospin mixing in the $^6\text{Li}^*(2^+)$ states lends credibility to this *ad hoc* mechanism.

Spin and parity restrictions for the $0^+ + 1^+ \rightarrow 0^+ + 0^+$ case hinder the reaction $^{12}\text{C}(d, \alpha_2)^{10}\text{B}$ independent of isospin conservation.²³ However, these restrictions allow us to use the partial-wave analysis developed by Jolivette and Richards²⁴ to determine unambiguously the J^π of a single isolated state of the intermediate nucleus, ^{14}N . The analysis is similar to that used for the $^{14}\text{N}(\alpha, \alpha_1)^{14}\text{N}$ (2.31) and $^{16}\text{O}(d, \alpha_1)^{14}\text{N}$ (2.31) reactions.^{7,11,24}

II. EXPERIMENTAL PROCEDURE

Deuterons (d) from an EN tandem Van de Graaff accelerator bombard a gaseous methane (CH_4) target of thickness $\leq 2 \text{ keV}$ in a differentially pumped gas scattering chamber. The experimental arrangements are the same as in Ref. 7 except for the following modifications: A 1.0 to 2.0- μA d^+ beam with angular divergence of $\pm 0.24^\circ$ passes

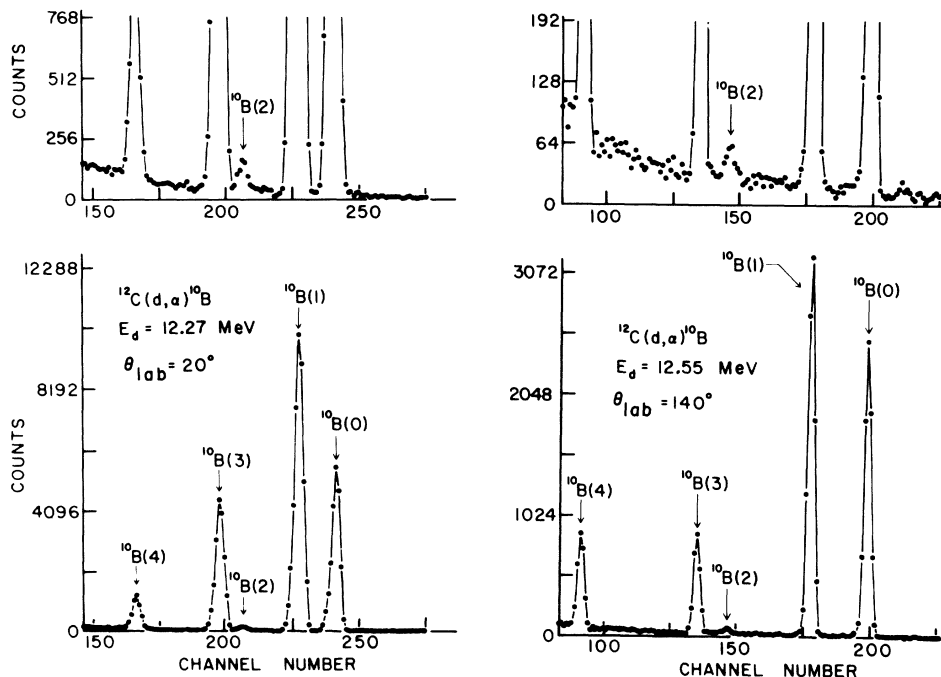


FIG. 1. Sample spectra for the reaction $^{12}\text{C}(d, \alpha_i)^{10}\text{B}(i)$. The α -particle groups are labeled by the corresponding final state in ^{10}B . The isospin-forbidden group is $^{10}\text{B}(2)$.

through the scattering chamber. An array of 8–13 Si surface-barrier solid-state detectors records the scattered α particles. We adjust the depletion depths of the solid-state detectors so that the pulse heights of the competing (d, p) and (d, d) reactions are smaller than that of any α -particle group of interest. The detector collimating slits have angular acceptances ranging from ± 1.53 to $\pm 2.15^\circ$. In general, each datum point represents the collection of 6000 μC of charge at a methane target gas pressure of 15 Torr.

Since the (d, α) reactions on ^{13}C and ^{16}O may result in contaminant peaks in the spectral region of interest, the ^{13}C and ^{16}O content in the methane target gas and the cross sections for the $^{13}\text{C}(d, \alpha)^{11}\text{B}$ and $^{16}\text{O}(d, \alpha)^{14}\text{N}$ reactions are of interest. Our directly measured $^{13}\text{C}/^{12}\text{C}$ isotopic ratio for the

methane target gas is consistent²⁵ with the natural-abundance value of 0.0112. At certain angles and energies the α_2 group from the reaction $^{12}\text{C}(d, \alpha_2)^{10}\text{B}$ may overlap α -particle groups from the $^{13}\text{C}(d, \alpha_i)^{11}\text{B}$ ($i=7-11$) reactions. No cross-section data exist for the $^{13}\text{C}(d, \alpha_i)^{11}\text{B}$ ($i=7-11$) reactions, but typical values for the (d, α_{1-3}) reaction on ^{13}C are 400 $\mu\text{b}/\text{sr}$.^{26,27} Using 400 $\mu\text{b}/\text{sr}$ as the maximum cross section for the $^{13}\text{C}(d, \alpha_i)^{11}\text{B}$ ($i=7-11$) reactions, the maximum possible contamination of our $^{12}\text{C}(d, \alpha)^{10}\text{B}$ data due to ^{13}C is 4 $\mu\text{b}/\text{sr}$. Reference 2 reports no α -particle group in their magnetic spectrograph spectra for 9 MeV $\leq E_d \leq 13$ MeV which corresponds to the $^{13}\text{C}(d, \alpha_i)^{11}\text{B}$ ($i=7-11$) reactions. We also do not observe any of these groups. The manufacturer states that the oxygen content of our methane target gas²⁸ is $^{16}\text{O}/^{12}\text{C} \approx 10^{-4}$. Jobst²⁹ observes 5 mb/sr as a maximum cross section for any of the $^{16}\text{O}(d, \alpha_i)^{14}\text{N}$ ($i=6-11$) reactions (8 MeV $\leq E_d \leq 9$ MeV). If we assume the same maximum as an upper limit for the $^{16}\text{O}(d, \alpha_i)^{14}\text{N}$ ($i=6-18$) reactions, then the ^{16}O contaminant

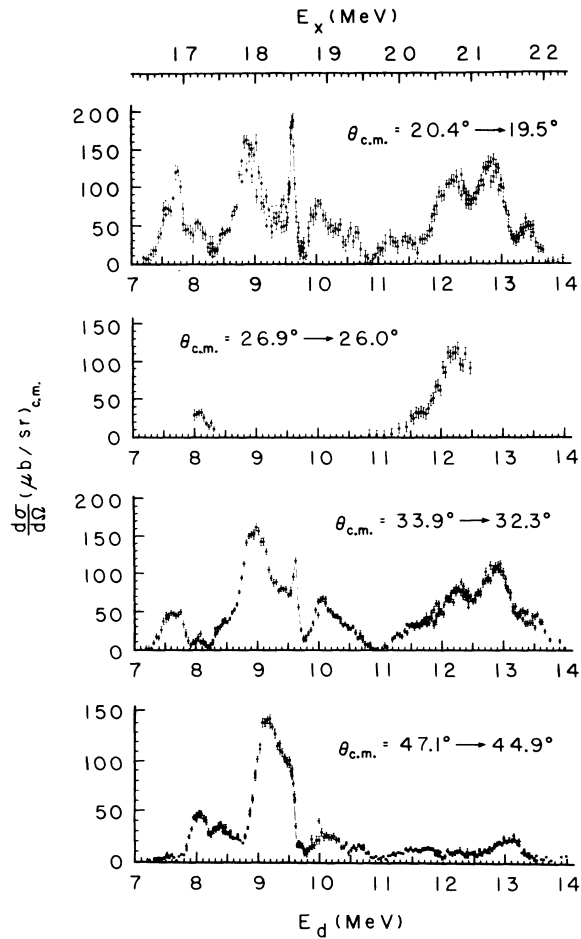


FIG. 2. $^{12}\text{C}(d, \alpha_2)^{10}\text{B}(1.74)$ cross sections (c.m.) versus laboratory deuteron energy (E_d) measured simultaneously at several fixed laboratory angles. The corresponding $\theta_{\text{c.m.}}$ is largest at the lowest E_d . The error bars represent only the statistical errors. The top scale gives the corresponding excitation energy (E_x) in ^{14}N .

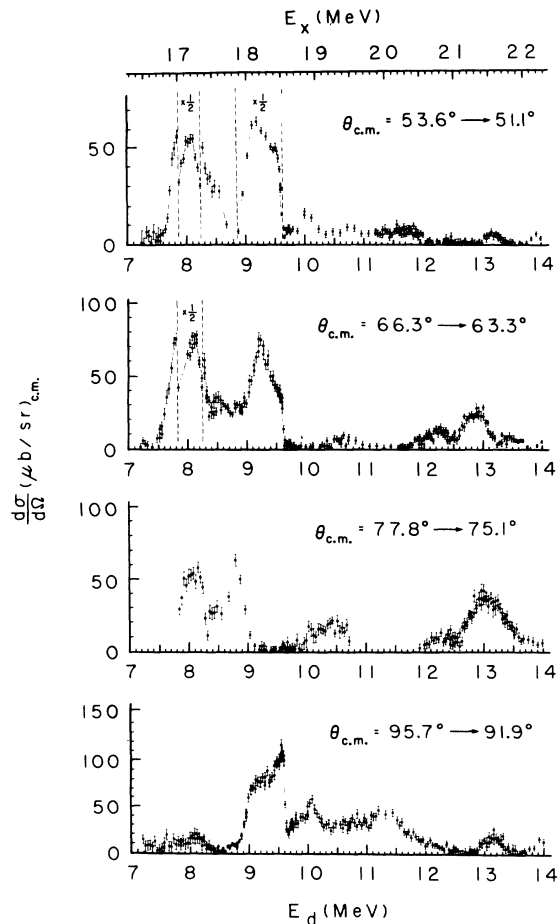


FIG. 3. Similar to Fig. 2 except different angles.

contributes at most only $0.5 \mu\text{b}/\text{sr}$ to our $^{12}\text{C}(d, \alpha)-^{10}\text{B}$ data at the overlap angles and energies. In fact, at no energy or angle do we observe any $^{16}\text{O}(d, \alpha)^{14}\text{N}$ groups.

Figure 1 shows typical α -particle spectra. The α_2 group has low yield (typically 1% of the nearby isospin-allowed groups); thus, accurate estimation of the background is important. (The background in the region of the α_2 group can arise from beam collimator slit-edge scattering, pileup between the elastic protons or deuterons and the α groups, and detector electronic noise.) We use a nonlinear least-squares computer program³⁰ to fit the background (assumed to be exponential) and the α_2 and α_3 peaks (assumed to be Gaussian). In fitting the spectra, the position of the α_2 group is fixed, the width of the α_2 group is set equal to that of the α_3 group, and the program varies the other Gaussian peak parameters (width of α_3 , position of α_3 , and areas of α_2 and α_3) and the background until χ^2 is minimized.

Since the cross sections for the reaction $^{12}\text{C}-$

$(d, \alpha_2)^{10}\text{B}$ are quite small, statistical uncertainties are the largest source of error for this channel. A detailed error analysis³¹ indicates that the systematic uncertainties in all the cross-section measurements may be as large as 2% with possibly another 2% random error in addition to the statistical errors. We note that the cross sections at all angles may be up to 0.4% low due to beam heating effects, and that the cross section at the four most forward angles (20, 26, 33, and 45° c.m.) may be up to 1% low due to pileup effects. The uncertainty in the absolute energy scale is placed at ± 15 keV. Reference 31 contains a detailed description of the experimental procedure.

III. RESULTS

The differential cross-section measurements consist of excitation functions taken simultaneously at 8–13 angles. Figures 2–5 exhibit the excitation functions for the isospin-forbidden α_2 channel.³² Figures 6–8 show samples of the (simultaneously recorded) excitation functions for the isospin-allowed

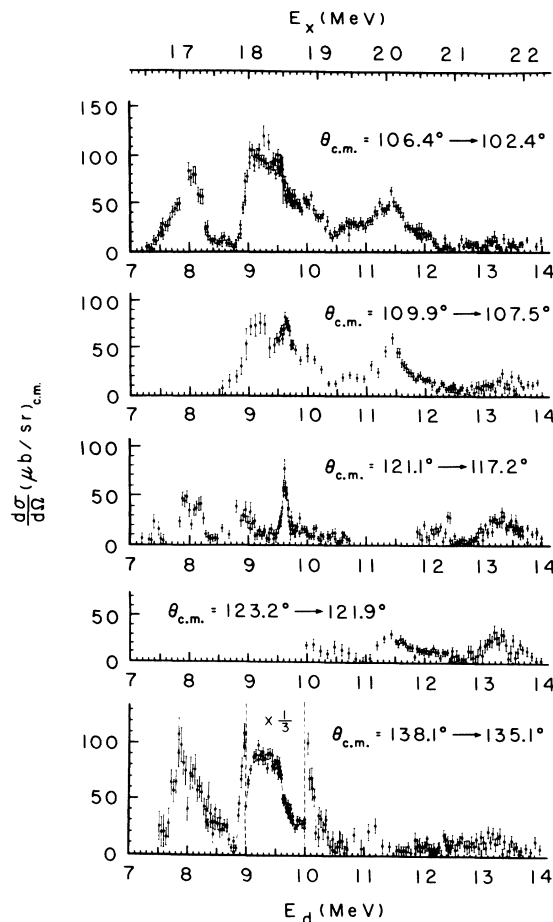


FIG. 4. Similar to Fig. 2 except different angles.

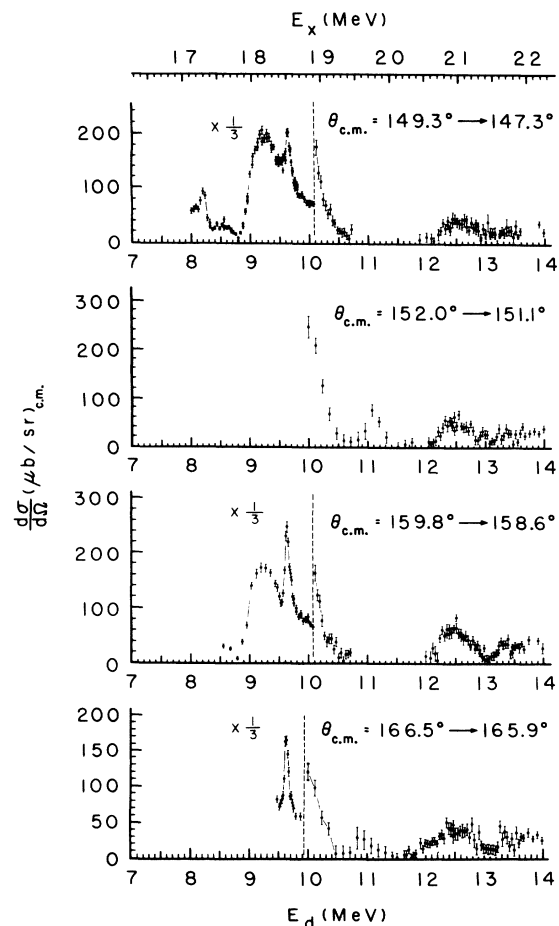


FIG. 5. Similar to Fig. 2 except different angles.

lowed α_0 , α_1 , and α_3 channels.³³ The deuteron bombarding energy E_d varies in 40-keV steps for $7.19 \text{ MeV} \leq E_d \leq 13.67 \text{ MeV}$ and 80-keV steps for $13.67 \text{ MeV} \leq E_d \leq 13.99 \text{ MeV}$. Because of the narrow resonance in the α_2 channel at $E_d = 9.61 \text{ MeV}$, E_d varies in 20-keV steps for $9.51 \text{ MeV} \leq E_d \leq 9.71 \text{ MeV}$. E_d in Figs. 2–8 is corrected for energy loss to the center of the target (the correction is $\sim 10 \text{ keV}$).

A few selected angular distributions for the isospin-forbidden α_2 channel are shown in Fig. 9. We obtain total cross sections for the α_0 , α_1 , and α_3 channels by fitting the angular distributions with a Legendre-polynomial expansion. The total cross sections for the α_2 channel are a result of the partial-wave analysis (see below). The total cross sections for the α_0 , α_1 , α_2 , and α_3 channels are shown in Fig. 10.

At many angles and energies the differential cross sections shown in Figs. 6–8 overlap previous $^{12}\text{C}(d, \alpha_{0,1,3})^{10}\text{B}$ measurements.^{2, 34, 35} Table I shows a comparison of the differential cross-section scale reported here and the scales reported in Refs. 2, 34, and 35. The agreement between the

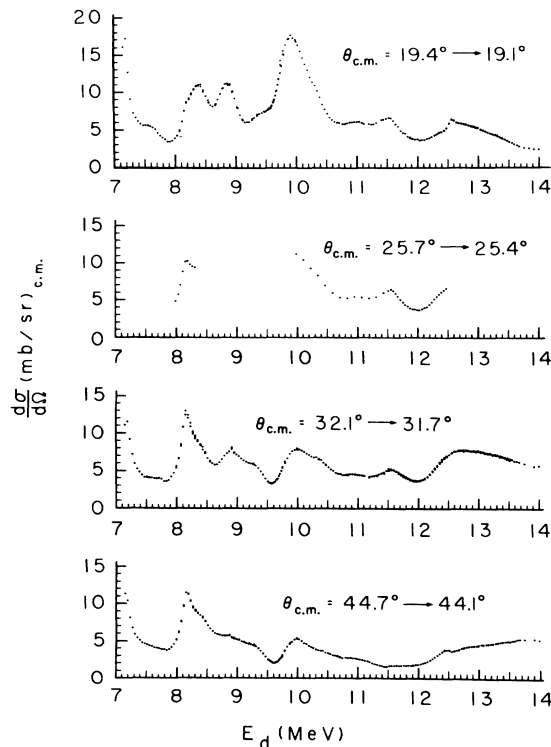


FIG. 6. A few of the $^{12}\text{C}(d, \alpha_0)^{10}\text{B}(\text{g.s.})$ cross sections (c.m.) vs laboratory deuteron energy (E_d) measured simultaneously at several fixed laboratory angles. The corresponding $\theta_{\text{c.m.}}$ is largest at the lowest E_d . The statistical errors are comparable to the size of the data points.

present scale and those of Refs. 34 and 35 is good. The discrepancy of approximately 40% between the present scale and that of Ref. 2 is a factor of 2 more than the reported systematic errors. Perhaps the discrepancy arises from the presence of narrow resonances in the $^{12}\text{C}(p, p_0)^{12}\text{C}$ excitation functions³⁶ near the energies, $E_p = 8.15$ and 9.27 MeV , that were used in Ref. 2 for target-thickness measurements. These resonances are not reported in the work of Nagahara,³⁷ which contains the $^{12}\text{C}(p, p_0)^{12}\text{C}$ cross sections used in Ref. 2 to set the differential cross section scale.

At some angles and energies the cross sections shown in Figs. 2–5 overlap the $^{12}\text{C}(d, \alpha_2)^{10}\text{B}$ data of Ref. 2 (but do not overlap the data of Ref. 3). In general, the agreement between the present data and that of Ref. 2 is good (when the cross section scale of Ref. 2 is corrected for the 40% discrepancy discussed above). However, there are

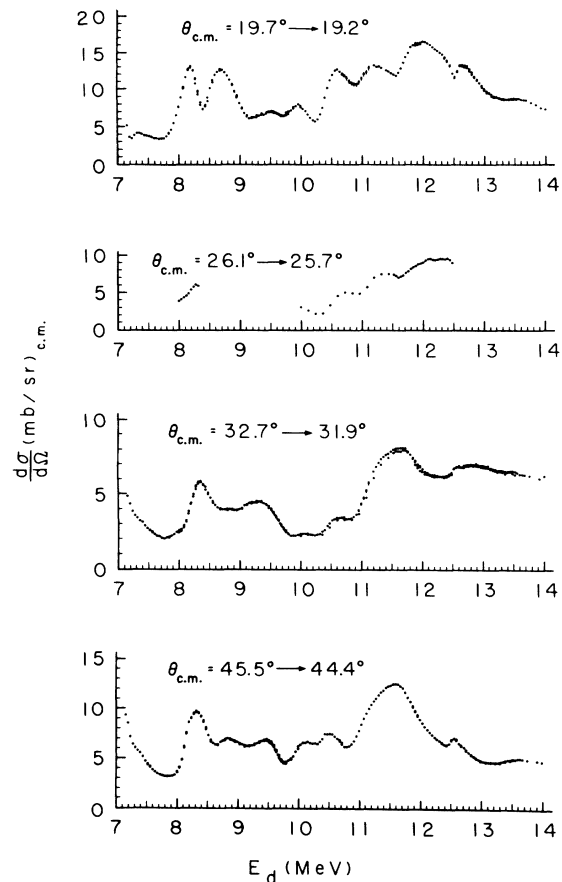


FIG. 7. A few of the $^{12}\text{C}(d, \alpha_1)^{10}\text{B}(0.717)$ cross sections (c.m.) vs laboratory deuteron energy (E_d) measured simultaneously at several fixed laboratory angles. The corresponding $\theta_{\text{c.m.}}$ is largest at the lowest E_d . The statistical errors are comparable to the size of the data points.

places where the two sets of α_2 data disagree even after the cross-section scale of Ref. 2 has been corrected. For example, for $9 \text{ MeV} \leq E_d \leq 10 \text{ MeV}$, $\theta_{\text{lab}} = 120^\circ$ ($\theta_{\text{c.m.}} \approx 137^\circ$), the present measurements are $\approx 100\%$ higher than those of Ref. 2. Also, at $E_d = 12.5 \text{ MeV}$, $150^\circ \leq \theta_{\text{c.m.}} \leq 160^\circ$, the present measurements are $\approx 400\%$ higher than those of Ref. 2. The sources of these discrepancies are unknown.

IV. DISCUSSION OF RESULTS

Violations of the isospin-selection rule may result from isospin impurities in the incoming channel, in the intermediate state, and/or the outgoing channel. Since the $T=1$ impurities of the ^{12}C ground state, the ^4He ground state, and the ^{10}B second excited state are estimated³⁸ to be 0.1,

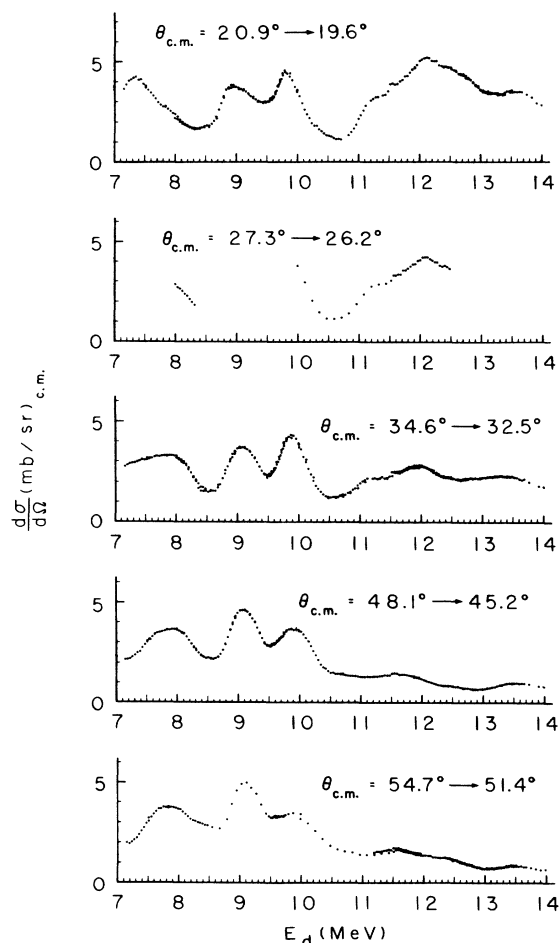


FIG. 8. A few of the $^{12}\text{C}(d, \alpha_2)^{10}\text{B}(2.15)$ cross sections (c.m.) vs laboratory deuteron energy (E_d) measured simultaneously at several fixed laboratory angles. The corresponding $\theta_{\text{c.m.}}$ is largest at the lowest E_d . The statistical errors are comparable to the size of the data points.

0.001, and 0.07%, respectively, and the $T=1$ impurity of the deuteron is expected to be negligible, direct reactions should introduce isospin impurities of only a few tenths of a percent for $^{12}\text{C}(d, \alpha_2)^{10}\text{B}$. Large isospin impurities in the intermediate states can result from the Coulomb force mixing nearby continuum states of the same J^π but differing isospin.¹⁴ Qualitatively, the cross sections due to direct effects vary slowly with energy, whereas those due to compound effects exhibit resonances which correspond to isospin-mixed intermediate states.

Single-step direct mechanisms with a single l transfer are also spin-parity forbidden for $^{12}\text{C}(d, \alpha_2)^{10}\text{B}$.³⁹ Multiple-step direct mechanisms are needed to account for nonzero cross sections. Estimates of the isospin impurities introduced by multistep direct mechanisms are on the order of a tenth of a percent.^{17, 19} Cross sections due to multistep direct mechanisms are, in general, expected to be slowly varying with energy, although broad resonant structure is predicted by mechanisms such as Noble's ^6Li mechanism.²¹

Our data indicate that the source of isospin mixing in the reaction $^{12}\text{C}(d, \alpha_2)^{10}\text{B}$ for $7.2 \text{ MeV} \leq E_d \leq 14.0 \text{ MeV}$ is ^{14}N intermediate states. The ratios of the isospin-forbidden α_2 total cross sections to the isospin-allowed α_0 , α_1 , and α_3 total cross sections (Fig. 10) are $\approx 1\%$, an order of magnitude larger than predicted by direct or multistep direct mechanisms. More significantly, relatively narrow resonances are present in the α_2 excitation functions (Figs. 2-5). These narrow resonances imply long-lived ^{14}N intermediate states as the source of the isospin impurity. The angular distributions for the α_2 channel (a few of which are shown in Fig. 9; also Fig. 1, Richards and Smith⁴⁰ and Fig. 3, Smith and Richards⁴¹) vary in symmetry about 90° c.m., sometimes being symmetric, but often being asymmetric in either the forward or backward directions. Below we will interpret the variation in fore-aft symmetry of the α_2 angular distributions in terms of interference effects between overlapping ^{14}N intermediate states of opposite parity. We confirm the conclusion² that for $^{12}\text{C}(d, \alpha_2)^{10}\text{B}$ a compound mechanism dominates the region $E_d \leq 11.3 \text{ MeV}$; we disagree with the conclusion^{2, 3} that a direct mechanism dominates the region $11.3 \text{ MeV} \leq E_d \leq 14 \text{ MeV}$. (In the region of disagreement between our interpretation and that of Refs. 2 and 3, our data are much more extensive.)

The α_0 , α_1 , and α_3 excitation functions exhibit (weak) fluctuations indicating that compound processes contribute to these channels. This is consistent with the findings of Klages, Baldeweg, and Stiller³⁴ that intermediate states are important for

$9 \text{ MeV} < E_d < 14 \text{ MeV}$. Individual resonances occur in these channels (e.g., the resonance(s) in the α_0 and α_1 channels near $E_d = 12.5 \text{ MeV}$, Figs. 6 and 7, and the resonance in the α_3 channel near $E_d = 11.5 \text{ MeV}$, Fig. 8) further verifying the importance of ^{14}N intermediate states.

V. ANALYSIS

Since our data indicate that the isospin impurity in the reaction $^{12}\text{C}(d, \alpha_2)^{10}\text{B}$ is introduced by ^{14}N intermediate states, the object of our analysis is to explain the α_2 cross sections with a suitable set of (isospin-mixed) ^{14}N states. In order to eliminate interference effects between overlapping, isospin-mixed ^{14}N states of differing J^π , we parame-

trize our α_2 data (Figs. 2–5) with S matrix elements (S_l 's) according to the prescription of Joliette and Richards²⁴:

$$\frac{d\sigma}{d\Omega} = (\chi^2/12) \left| \sum_l \frac{2l+1}{[l(l+1)]^{1/2}} S_l \frac{dP_l(\cos\theta)}{d\theta} \right|^2. \quad (1)$$

References 7, 24, and 31 contain a detailed discussion of the fitting procedure. We interpret a resonance in the l th partial wave as a ^{14}N level with $J^\pi = l^{(-1)^l}$.

There exist $2^{l_{\text{max}}-2}$ degenerate sets of S_l 's (each set is called a "solution") which give identical fits to the angular distributions.²⁴ The amplitude of the l_{max} th partial wave is unique – the degeneracy

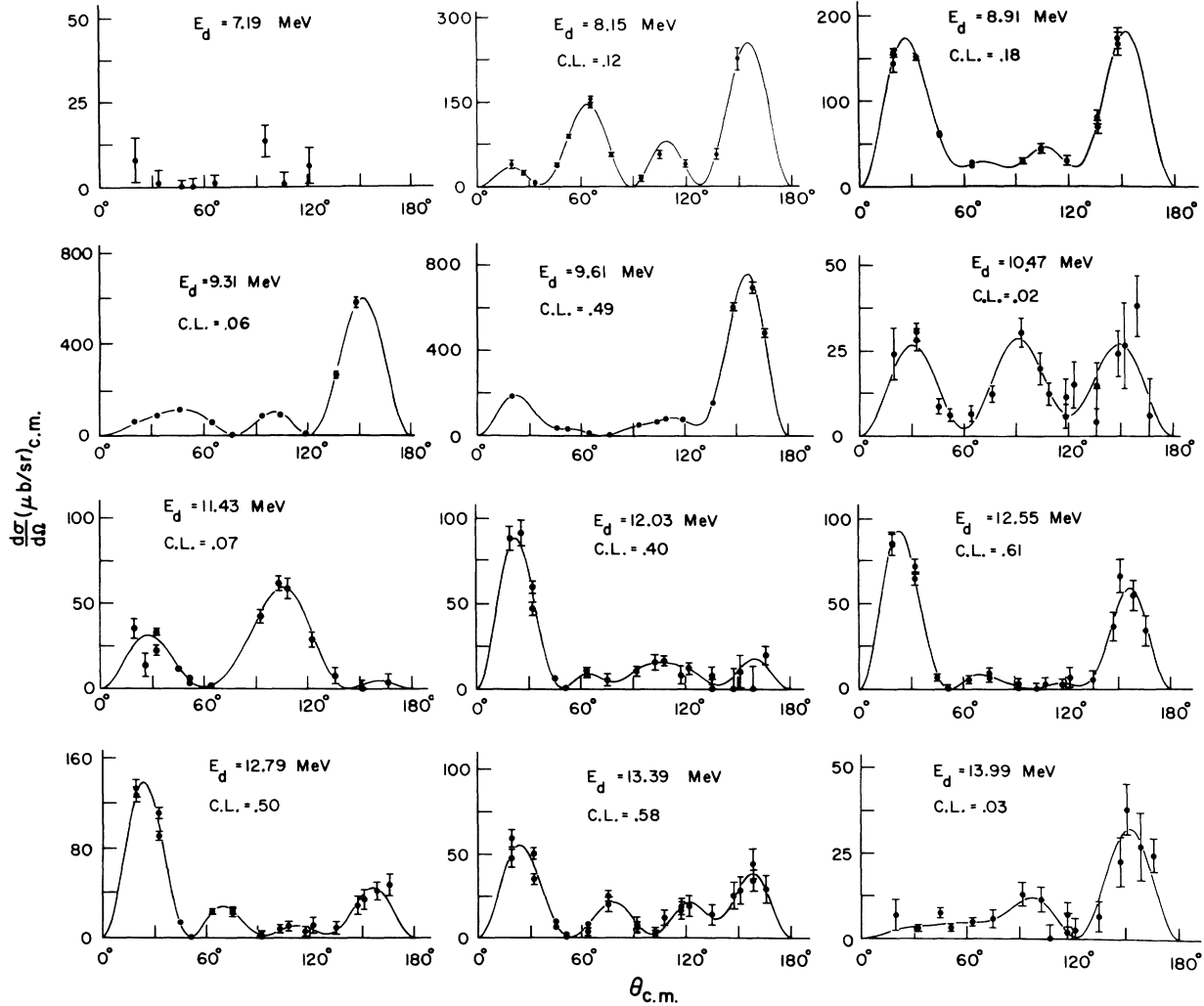


FIG. 9. Some selected angular distributions for the reaction $^{12}\text{C}(d, \alpha_2)^{10}\text{B}(1.74)$. The solid line is the partial-wave fit to the data. Ordinary spin-parity restrictions require $d\sigma/d\Omega$ to vanish at 0 and 180° (see Refs. 6 and 24). Confidence levels (C.L.: the probability that another measurement would result in a larger χ^2) between 0.10 and 0.90 are acceptable.

is in the other $l_{\max} - 1$ partial waves. The highest l_{\max} that we require to obtain acceptable fits to our data is 5; thus, we have eight degenerate sets of S_l 's from which to choose the "physical" solution. One simplification arises, namely the $2^{l_{\max}-2}$ solutions tend to pair into $2^{l_{\max}-3}$ solutions which differ substantially in amplitude of the partial waves. Table II illustrates this pairing. The eight ambiguous solutions "pair" into only four solutions with substantially different S matrix elements. Thus, we are left with four solutions from which to choose the "physical" solution.

The criterion that we use to choose the "physical" solution from the four degenerate solutions is based on the prediction¹⁵ that isospin conservation in reactions involving intermediate states of increasing excitation is spin-dependent, being re-established first for the lowest-spin states. For

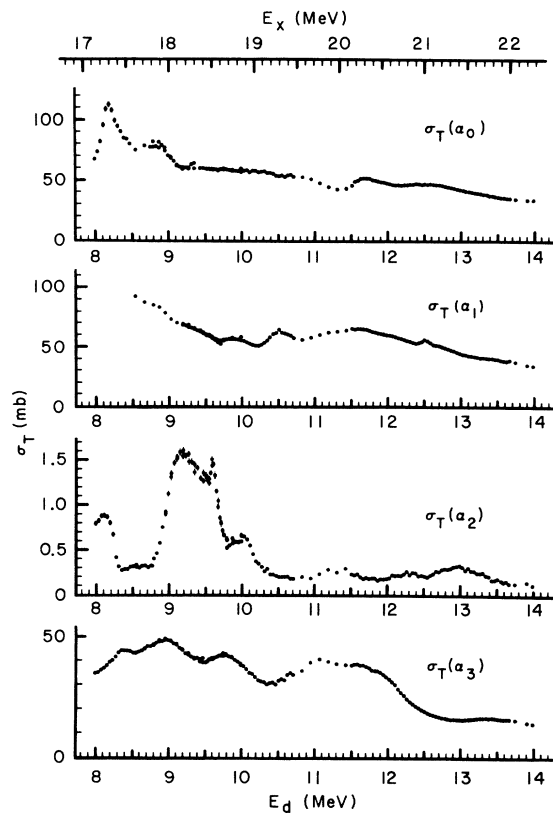


FIG. 10. Total cross sections for the $^{12}\text{C}(d, \alpha_{0-3})^{10}\text{B}$ reactions as a function of deuteron bombarding energy. The total cross sections for the α_0 , α_1 , and α_3 groups result from fitting the angular distributions with a Legendre-polynomial expansion. The total cross sections for the α_2 group come from the partial-wave analysis of the angular distributions:

$$\sigma_T(\alpha_2) = (\pi \lambda^2 / 3) \sum_l (2l + 1) S_l^2.$$

The top scale gives the corresponding excitation energy, E_x , in ^{14}N .

$20.7 \text{ MeV} \leq E_x \leq 22.2 \text{ MeV}$ ($12.2 \text{ MeV} \leq E_d \leq 14.0 \text{ MeV}$), we find that two of the four degenerate solutions have, on the average, substantially smaller $|S_1|$ and $|S_2|$. The two preferred solutions are Sets I, II and III, IV of Table II (although Set VII, VIII in Table II has essentially the same $|S_1|$ and $|S_2|$ as Set I, II; Set I, II has lower $|S_1|$ and $|S_2|$ over most of the range $20.7 \text{ MeV} \leq E_x \leq 22.2 \text{ MeV}$). On the basis of the above criterion we believe that one of these two preferred solutions corresponds to the "physical" solution (we have no reason for choosing between them). The two preferred solutions are identical for $8.0 \text{ MeV} \leq E_d \leq 9.4 \text{ MeV}$, and are qualitatively similar for $9.4 \text{ MeV} \leq E_d \leq 14 \text{ MeV}$. One of the two preferred solutions, solution Set I, II of Table II, is shown in Fig. 2 of Ref. 40.

We point out that (1) it is difficult to guarantee that one stays with the same solution as the energy changes⁴² and (2) our criterion for choosing the "physical" solution differs from Jolivet's criterion⁴² (Jolivet's criterion is to choose the solution which implies the fewest resonant states). Such a criterion may not pick one of our two preferred solutions as the physical solution. Indeed, Jolivet finds that the "physical" solution for his $^{16}\text{O}(d, \alpha_1)^{14}\text{N}(2.31)$ data implies large $|S_1|$ and $|S_2|$ for high ^{18}F excitation energy.⁴³ The giant dipole resonance may enhance the contribution from 1^- states at these energies.

The bulk of the ^{14}N level assignments from our $^{12}\text{C}(d, \alpha_2)^{10}\text{B}$ data (shown in Table III) are obtained from a visual inspection of the two preferred solutions discussed above. We demand consistency between the two preferred solutions in making a level assignment. Despite the above warnings, we believe the J^π assignments are unambiguous. There is, of course, no ambiguity if the resonance occurs in the l_{\max} th partial wave or if, for $l < l_{\max}$, all solutions show the resonance (this is generally true for $l \geq 3$). For those resonances where $l < l_{\max}$, the locations and widths implied by

TABLE I. Comparison of $^{12}\text{C}(d, \alpha_{0,1,3})^{10}\text{B}$ differential cross-section scales.

Reference	Reported systematic errors (%)	$\frac{(d\sigma/d\Omega)_{\text{Ref.}} - (d\sigma/d\Omega)_{\text{Present}}}{(d\sigma/d\Omega)_{\text{Present}}}$
2	20	-0.4 ^a
34	20-25	+0.15 ^a
35	16	+0.07 ^b
Present work	2	...

^a From graphs in this reference.

^b From cross sections supplied by the authors of this reference.

the different solutions often vary, causing these quantities to be more uncertain than for $l = l_{\max}$. In addition to these problems, interference effects in a single partial wave (interference effects between overlapping ^{14}N states of the same J^π) are large. The presence of these interference effects is confirmed by the preliminary results of fitting the partial waves in Fig. 2 of Ref. 40 with a multi-level expansion.⁴⁴ An extensive reexamination of our partial-wave analysis to insure continuity of solutions and to check our choice of a physical solution (by using Jolivet's criteria) is underway. The results of the multilevel fitting of the partial waves of the physical solution will be presented in a future publication.

The ^{14}N level assignment at $E_x = 16.9$ MeV, shown as (5^-) in Table III occurs in an energy region ($7.67 \text{ MeV} \leq E_d \leq 7.91 \text{ MeV}$) where we cannot successfully parametrize the α_2 data with $l_{\max} = 4$ and in which we have too few angles to allow $l_{\max} = 5$. While this result only implies that the ^{14}N resonance at $E_x = 16.9$ MeV (indicated by the sharp peak in the 20° excitation function at $E_d = 7.8$ MeV, Fig. 2) has natural spin-parity $\geq 5^-$, the qualitative behavior of this peak as a function of angle suggests $J^\pi = 5^-$. For $E_d < 7.67$ MeV the data are successfully parametrized with $l_{\max} = 4$ and imply uniquely

that the peak at $E_d \approx 7.6$ MeV at $\theta_{\text{c.m.}} \approx 20$ and 34° (Fig. 2) arises from a 4^+ level in ^{14}N at $E_x = 16.8$ MeV.

The α_2 channel is sensitive only to those ^{14}N states that have natural parity and that are isospin-mixed ($T=0$ states with $T=1$ impurity or vice-versa). Hence we expect to observe only a very few of the existing ^{14}N states via the α_2 channel. Indeed, we find that 15 ^{14}N states (Table III) qualitatively account for most of the α_2 cross sections in the 6 MeV excitation region studied. The average ^{14}N level spacing, D , as observed via the α_2 channel, is $D \approx 400$ keV. The average half width of these levels, Γ , is $\Gamma \approx 400$ keV. Thus, $\Gamma \approx D$, and the average ^{14}N level spacing, as observed in the α_2 channel, is intermediate to the region of individual isolated resonances where $\Gamma \ll D$ and the statistical region where $\Gamma \gg D$. In this intermediate region, unlike the individual resonance region, each angular distribution is not required to be symmetric about 90° c.m. Since positive-parity states and negative-parity states are about equal in number in the α_2 channel, as often as not overlapping states in the α_2 channel have opposite parity. If interference between such overlapping states of opposite parity occurs, asymmetric angular distributions result. Asymmetries in the angular dis-

TABLE II. "Paired" degenerate sets of S -matrix elements for $^{12}\text{C}(d, \alpha_2)^{10}\text{B}$. These eight degenerate solution sets are obtained at $E_d = 12.43$ MeV, where $l_{\max} = 5$. The S matrix elements (S_l) are parametrized according to $S_l = \rho_l e^{i\phi_l}$, with $\phi_{l_{\max}} \equiv 0$. Note that each solution set on the left is almost identical to the solution set in the corresponding position on the right. For the physical reasons discussed in the text, we choose the two "paired" solution Sets I, II and III, IV as candidates for the "physical" solution (we have no basis for choosing between the two preferred solutions). Solution Set I, II is shown in Fig. 2 of Ref. 40.

Solution Set	l	ρ_l	ϕ_l (radians)	Solution Set	l	ρ_l	ϕ_l (radians)
I	1	0.0102	5.848	II	1	0.0110	5.842
	2	0.0176	0.919		2	0.0176	0.874
	3	0.0166	0.078		3	0.0170	0.053
	4	0.0334	1.442		4	0.0332	1.441
	5	0.0198	0.000		5	0.0198	0.000
III	1	0.0065	4.839	IV	1	0.0072	4.783
	2	0.0047	1.399		2	0.0038	1.465
	3	0.0405	6.081		3	0.0404	6.071
	4	0.0154	4.997		4	0.0156	4.992
	5	0.0198	0.000		5	0.0198	0.000
V	1	0.0230	6.165	VI	1	0.0225	6.144
	2	0.0034	3.450		2	0.0042	3.546
	3	0.0290	5.955		3	0.0288	5.938
	4	0.0265	4.875		4	0.0269	4.874
	5	0.0198	0.000		5	0.0198	0.000
VII	1	0.0119	4.087	VIII	1	0.0122	4.153
	2	0.0166	0.998		2	0.0162	0.954
	3	0.0331	0.002		3	0.0333	6.274
	4	0.0221	1.375		4	0.0219	1.373
	5	0.0198	0.000		5	0.0198	0.000

tributions are observed (Fig. 9, also Fig. 1 of Ref. 40). These asymmetries (sometimes forward peaking, sometimes backward peaking) persist for energy intervals up to four times the average half width (Fig. 3 of Ref. 40). Apparently the relative phases between the ^{14}N levels involved have values which produce these intervals of asymmetry.

From the ratio, $R [= \sigma_T(\alpha_2)/\sigma_T(\alpha_i)]$, of the isospin-forbidden to isospin-allowed total cross sections (Fig. 10) and the inhibition factor, I.F., which corrects R for angular momentum, parity, and penetrability restrictions (I.F. is obtained from a Hauser-Feshbach calculation for $E_x = 19.7$ MeV²), we estimate a lower limit to the isospin impurity, $\beta^2 [= R/(R + \text{I.F.})]$, of some individual levels observed in the α_2 channel. The isospin-impurity estimate is a lower limit because we assume that only compound processes contribute to the isospin-allowed channels. The estimate is typically $\approx 10\%$, e.g., the estimate for the 4^+ level at $E_x = 17.2$ MeV is $\beta^2 \approx 9\%$.³¹ An additional correction for the relative densities of $T=0$ and $T=1$ states allows us to estimate the lower limit for the average isospin impurity, $\langle \beta^2 \rangle \{= \frac{4}{3}[-1 + (1 + R/\text{I.F.})^{1/2}]\}$, of all the ^{14}N resonances that we observe in the α_2 channel. This lower limit is 4% .³¹

One may hope to determine the isospin composition (predominantly $T=0$ with some $T=1$ impurity or vice versa) of the ^{14}N levels that we assign from the α_2 data by comparing them with $T=0$ and $T=1$ ^{14}N levels and with $T=1$ ^{14}C and ^{14}O levels

TABLE III. ^{14}N levels implied by the present α_2 data and our partial-wave analysis. Parentheses around level parameter assignments indicate uncertainty in the enclosed quantity. Resonant energies and widths are approximate only. (See text for a discussion of ambiguous solution problems.)

E_d (MeV)	E_x (MeV)	J^π	$\Gamma_{\text{c.m.}}$ (keV)
7.6	16.8	4^+	~ 300
7.8	16.9	(5^-)	~ 100
8.1	17.2	4^+	~ 300
9.1	18.1	$(1^-, 2^+)$	(~ 300)
9.2	18.1	4^+	~ 600
9.3	18.2	3^-	(~ 400)
9.5	18.4	3^-	(~ 300)
9.61	18.50	5^-	~ 60
10.0	18.8	4^+	(~ 400)
11.5	20.1	1^-	(~ 500)
12.3	20.8	5^-	~ 600
12.3	20.8	$(3^-, 4^+)$	(~ 500)
12.9	21.3	4^+	$(\sim 1000)^a$
13.1	21.5	3^-	(~ 500)
13.4	21.7	5^-	~ 200

^a May be more than one 4^+ level.

for the corresponding ^{14}N excitation energy range. This approach is not successful, since either spin and parity information is generally lacking for the ^{14}C , ^{14}N , and ^{14}O levels in the region of interest or the reported levels have unnatural spin and parity⁴⁵ (only natural-parity levels may decay via the α_2 channel).

The 1^- level that we observe in the α_2 channel at $E_x = 20.1$ MeV may account for the difference in the $^{14}\text{N}(\gamma, p)^{13}\text{C}$ and $^{14}\text{N}(\gamma, n)^{13}\text{N}$ cross sections observed near $E_x = 20$ MeV.^{46, 47} When the differential cross sections for these two reactions are plotted on the same graph (Fig. 2 of Ref. 47), they differ substantially in the region of $E_x = 20$ MeV. This behavior we expect if the (γ, p) and (γ, n) reactions proceed via a ^{14}N state which is primarily $T=1$ with some $T=0$ impurity.⁴⁸ (0^- , 1^- , and 2^- ^{14}N states can be excited via the $E1$ giant dipole resonance.) We tentatively identify this isospin-mixed ^{14}N state as the 1^- level we observe at 20.1 MeV.

We find some evidence for grouping of ^{14}N states of the same J^π for $3 \leq J \leq 5$. Levels which appear to group are the two 3^- levels at $E_x = 18.2$ and 18.4 MeV; the 4^+ levels at $E_x = 16.8$, 17.2, 18.1, and 18.8 MeV; a possible cluster of 4^+ levels near $E_x \approx 21.3$ MeV; and the two 5^- levels at 20.8 and 21.7 MeV. One explanation for grouping of two or more isospin-mixed levels of the same J^π is that the levels have appreciable mirror configurations (similar to the famous ^8Be 2^+ levels at 16.6 and 16.9 MeV¹⁶). Another explanation for grouping is that two or more unrelated states of the same J^π and different isospin accidentally overlap, their isospins being mixed by the Coulomb force. For such unrelated states, the incoming and outgoing partial widths are also unrelated. Hence, it is possible that one (or more) of the states does not have an observable cross section. This might explain why some resonances in the partial waves are isolated; e.g., the 5^- resonance at $E_x = 18.50$ MeV (Fig. 2 of Ref. 40).

Noble's ^6Li mechanism²¹ fails to explain our α_2 data.⁴¹ The failure of Noble's ^6Li mechanism to explain the "fine" structure reported in Ref. 41 led Weller⁴⁹ to modify the ^6Li mechanism by coupling the $^6\text{Li}^*$ and ^8Be "intermediate" nuclei to a state of definite angular momentum, L . If $L \neq 0$, multiplets result. In particular, if $L=3$, then intermediate states of $J^\pi = 1^-, 3^-,$ and 5^- result with a center of gravity near $E_x = 20.8$ MeV. Our analysis indicates six ^{14}N levels in the region where Weller's model predicts only three. This, coupled with the fact that there appears to be no *a priori* reason to choose only $L=3$ for the $^8\text{Be} + ^6\text{Li}^*$ cluster indicates to us that evidence supporting Weller's model is still lacking. Indeed, recent

measurements indicate the intensity of the isospin mixing of the $^6\text{Li}^* 2^+$ states ($0.008^{+0.60}_{-0.008}$ from Debevec, Garvey, and Hingerty,⁵⁰ ≤ 0.005 from Cocco and Adloff⁵¹) is small, perhaps small enough to make isospin-mixing mechanisms involving them unimportant.⁵¹

VI. CONCLUSIONS

We conclude that for $7.2 \text{ MeV} \leq E_d \leq 14.0 \text{ MeV}$ isospin impurities are introduced into the reaction $^{12}\text{C}(d, \alpha_2)^{10}\text{B}$ by relatively few isospin-mixed ^{14}N intermediate states. In agreement with measurements on other isospin-violating reactions,⁶⁻¹¹ we

see no evidence for significant contributions from direct- or semidirect-reaction processes.

ACKNOWLEDGMENTS

We gratefully acknowledge the support and encouragement of Professor H. T. Richards throughout the course of this work. Particular thanks go to Dr. J. Nickles, Dr. D. Pledger, Dr. P. L. Jolivet, S. Wilson, G. Klody, N. Magee, and D. Sandin for assistance in data acquisition, to Dr. P. L. Jolivet for the use of several computer programs, and to Professor C. H. Blanchard for several helpful discussions.

*Work supported in part by the U. S. Atomic Energy Commission.

¹See C. P. Browne, in *Isobaric Spin in Nuclear Physics*, edited by J. D. Fox and D. Robson (Academic, New York, 1966), p. 136, for a review of the literature up to 1966.

²L. Meyer-Schützmeister, D. von Ehrenstein, and R. G. Allas, *Phys. Rev.* **147**, 743 (1966).

³J. Jänecke, T. F. Yang, R. M. Polichar, and W. S. Gray, *Phys. Rev.* **175**, 1301 (1968).

⁴P. G. Bizzeti and A. M. Bizzeti-Sona, *Nucl. Phys.* **A108**, 274 (1968).

⁵R. M. Polichar, J. Jänecke, T. F. Yang, and W. S. Gray, *Bull. Am. Phys. Soc.* **13**, 1425 (1968).

⁶J. Jobst, S. Messelt, and H. T. Richards, *Phys. Rev.* **178**, 1663 (1969).

⁷P. B. Tollefsrud and P. L. Jolivet, *Phys. Rev. C* **1**, 398 (1970).

⁸J. R. Duray and C. P. Browne, *Phys. Rev. C* **1**, 776 (1970).

⁹A. Richter, L. Meyer-Schützmeister, J. C. Stoltzfus, and D. von Ehrenstein, *Phys. Rev. C* **2**, 1361 (1970).

¹⁰C. M. Chesterfeld and P. D. Parker, *Bull. Am. Phys. Soc.* **15**, 1654 (1970).

¹¹P. L. Jolivet, Ph.D. thesis, University of Wisconsin, 1970 (unpublished), available through University Microfilms, Inc., Ann Arbor, Michigan.

¹²J. Jänecke, T. F. Yang, W. S. Gray, and R. M. Polichar, *Phys. Rev. C* **3**, 79 (1971).

¹³H. Moringa, *Phys. Rev.* **97**, 444 (1955).

¹⁴D. H. Wilkinson, *Phil. Mag.* **1**, 379 (1956).

¹⁵A. M. Lane and R. G. Thomas, *Rev. Mod. Phys.* **30**, 257 (1958).

¹⁶J. B. Marion, *Phys. Letters* **14**, 315 (1965).

¹⁷R. J. Drachman, *Phys. Rev. Letters* **17**, 1017 (1966).

¹⁸T. A. Griffy, *Phys. Letters* **21**, 693 (1966).

¹⁹J. V. Noble, *Phys. Rev.* **162**, 934 (1967).

²⁰J. V. Noble, *Phys. Rev.* **173**, 1034 (1968).

²¹J. V. Noble, *Phys. Rev. Letters* **22**, 473 (1969).

²²A. I. Baz and V. I. Manko, *Phys. Letters* **28B**, 541 (1969).

²³Y. Hashimoto and W. P. Alford, *Phys. Rev.* **116**, 981 (1959).

²⁴P. L. Jolivet and H. T. Richards, *Phys. Rev.* **188**, 1660 (1969).

²⁵Measured by G. Parr, Mass Spectrometry Service,

Department of Chemistry, University of Wisconsin, Madison.

²⁶J. R. Curry, W. R. Coker, and P. J. Riley, *Phys. Rev.* **185**, 1416 (1969).

²⁷R. Klages, F. Baldweg, V. Bredel, H. Guratzsch, G. Stiller, and S. Tesch, *Nucl. Phys.* **A152**, 232 (1970).

²⁸Methane ultra high purity gas. Obtained from Matheson Gas Products, Joliet, Illinois.

²⁹J. E. Jobst, *Phys. Rev.* **168**, 1156 (1968).

³⁰Program PKFITS. See F. deForest, Ph.D. thesis, University of Wisconsin, 1967 (unpublished), available through University Microfilms, Inc., Ann Arbor, Michigan.

³¹H. V. Smith, Jr., Ph.D. thesis, University of Wisconsin, 1970 (unpublished), available through University Microfilms, Inc., Ann Arbor, Michigan.

³²For a tabulation of the α_2 cross-section values, order document NAPS 01846 from ASIS, National Auxiliary Publications Service, c/o CCM Information Corporation, 866 Third Avenue, New York, New York, 10022, remitting \$2.00 for each microfiche or \$5.00 for each photocopy.

³³To obtain figures of the α_0 , α_1 , and α_3 excitation functions measured but not shown in Figs. 6-8, plus a tabulation of the α_0 , α_1 , and α_3 cross-section values, order document NAPS 01847 from ASIS, National Auxiliary Publications Service, c/o CCM Information Corporation, 866 Third Avenue, New York, New York, 10022, remitting \$4.00 for each microfiche or \$10.50 for each photocopy.

³⁴R. Klages, F. Baldweg, and G. Stiller, *Nucl. Phys.* **A121**, 113 (1968).

³⁵H. Cords, G. U. Din, and B. A. Robson, *Nucl. Phys.* **A127**, 95 (1969).

³⁶A. C. L. Barnard, J. B. Swint, and T. B. Clegg, *Nucl. Phys.* **86**, 130 (1966).

³⁷Y. Nagahara, *J. Phys. Soc. Japan* **16**, 133 (1961).

³⁸W. M. MacDonald, in *Nuclear Spectroscopy*, edited by F. Ajzenberg-Selove (Academic, New York, 1960), Pt. B, p. 943.

³⁹T. Yanabu, *J. Phys. Soc. Japan* **16**, 2118 (1961).

⁴⁰H. T. Richards and H. V. Smith, Jr., *Phys. Rev. Letters* **27**, 1735 (1971).

⁴¹H. V. Smith, Jr., and H. T. Richards, *Phys. Rev. Letters* **23**, 1409 (1969).

- ⁴²P. L. Jolivette, *Phys. Rev. Letters* **26**, 1383 (1971).
⁴³P. L. Jolivette, Ph.D. thesis, University of Wisconsin, 1971 (unpublished), available through University Microfilms, Inc., Ann Arbor, Michigan.
⁴⁴D. Steck, private communication.
⁴⁵F. Ajzenberg-Selove, *Nucl. Phys.* **A152**, 1 (1970).
⁴⁶J. D. King, R. N. H. Haslam, and R. W. Parsons, *Can. J. Phys.* **38**, 231 (1960).
⁴⁷R. Kosiek, K. Maier, and K. Schläpman, *Phys. Letters* **9**, 260 (1964).
⁴⁸F. C. Barker and A. K. Mann, *Phil. Mag.* **2**, 5 (1957).
⁴⁹H. R. Weller, *Phys. Rev. C* **2**, 321 (1970).
⁵⁰P. T. Debevec, G. T. Garvey, and B. E. Hingerty, *Phys. Letters* **34B**, 497 (1971).
⁵¹C. L. Cocke and J. C. Adloff, *Nucl. Phys.* **A172**, 417 (1971).

PHYSICAL REVIEW C

VOLUME 6, NUMBER 2

AUGUST 1972

Asymmetric Proton Yields from the Sequential Reaction ${}^6\text{Li}({}^3\text{He}, \alpha p){}^4\text{He}^\dagger$

D. T. Thompson* and G. E. Tripart

Department of Physics, Washington State University, Pullman, Washington 99163

(Received 24 February 1972)

Measurements have been made of the asymmetric proton yields about the ${}^5\text{Li}$ recoil direction using the sequential reaction ${}^6\text{Li}({}^3\text{He}, \alpha p){}^4\text{He}$ for both the ground and first excited states of ${}^5\text{Li}$ at a beam energy of 1.54 MeV. Measurements were made out of the reaction plane, and the results are in qualitative agreement with the predictions of a model proposed by Reimann, Martin, and Vogt. Distorted-wave Born-approximation stripping theory may also be capable of explaining the asymmetric results.

I. INTRODUCTION

Reactions between light nuclei which produce three particles at low bombarding energy have been the subject of considerable experimental and theoretical investigation since about 1965.^{1,2} Even though these experiments are complicated by difficult kinematics and experimental uncertainties, it has recently been possible to observe some important phenomena and to extract quantitative results concerning nuclear structure³⁻⁵ and nuclear reactions.⁶⁻⁸

This paper will be concerned with a sequential reaction leading to three final-state particles of the general form

$$B + T \rightarrow 1 + I \rightarrow 1 + 2 + 3, \quad (1)$$

where B represents the beam nucleus, T the target nucleus, 1 the first-emitted particle, and 2 and 3 the particles resulting from the spontaneous breakup of the intermediate nucleus I . The form of (1) implies that the reaction proceeds through a stripping or a pickup process, as opposed to the reaction

$$B + T \rightarrow C \rightarrow 1 + I \rightarrow 1 + 2 + 3,$$

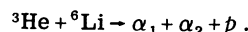
in which a compound-nucleus C is formed.

There are three coordinate systems which must be defined: (1) The laboratory system (lab) is the coordinate system in which the target nucleus is at rest; (2) the system center-of-mass (scm) system

is the coordinate system in which the vector momentum of the beam and target nuclei is zero; and (3) the recoil center-of-mass system (rcm) is the coordinate system in which the recoil nucleus I is at rest.

The transformations and kinematic correction factors among these coordinate systems have been previously derived^{4, 8-10} and will not be presented here. Throughout this discussion spherical polar coordinates will be used with the polar axis parallel with and in the direction of the beam.

The particular reaction which is the object of this study is the reaction



Measurements of two of the final-state particles in coincidence are kinematically restricted to certain loci in the E_1 - E_2 plane as shown in Fig. 1. Since this reaction has previously been determined¹¹⁻¹³ to proceed sequentially via the states of ${}^8\text{Be}$ and ${}^5\text{Li}$ which are kinematically allowed, the open three-body channels are

$${}^3\text{He} + {}^6\text{Li} \rightarrow \alpha_1 + {}^5\text{Li}(\text{g.s.}) \quad Q = 14.9137 \text{ MeV}, \quad (2a)$$

$${}^3\text{He} + {}^6\text{Li} \rightarrow \alpha_1 + {}^5\text{Li}^*(7.5) \quad Q = 7.4 \text{ MeV}, \quad (2b)$$

$${}^3\text{He} + {}^6\text{Li} \rightarrow p + {}^8\text{Be}(\text{g.s.}) \quad Q = 16.7869 \text{ MeV}, \quad (2c)$$

$${}^3\text{He} + {}^6\text{Li} \rightarrow p + {}^8\text{Be}^*(2.9) \quad Q = 13.9 \text{ MeV}, \quad (2d)$$